Distinct Impacts of Land Use and Land Management on Summer Temperatures

Liang Chen[1,2]* and Paul A. Dirmeyer[2]

[1] *Climate and Atmospheric Sciences Section, Illinois State Water Survey, Prairie Research Institute, University of Illinois at Urbana-Champaign, Champaign, IL, United States,* [2] *Center for Ocean-Land-Atmosphere Studies, George Mason University, Fairfax, VA, United States*

Land use has been recognized as an important anthropogenic forcing of climate change in recent studies. However, climatic effects of land management practices have been little discussed and compared to land-use impacts. As land-atmosphere interactions via surface fluxes are particularly strong during the warm season, we investigate the impacts of historical land use and present irrigation practices on summer temperatures in the Northern Hemisphere using the most recent version of Community Earth System Model. Our results suggest that historical land use leads to an overall cooling in the middle latitudes and a warming in the tropics, and the sign and magnitude of the changes in temperature depend on the type of land cover change. On the other hand, summer irrigation leads to a significant cooling over many irrigated areas due to enhanced evapotranspiration, and the local cooling is comparable to and even stronger than the land-use effects. Both land use and irrigation can also significantly influence the intensity and frequency of hot extremes. Land use shows stronger impacts during the night through ground heat flux feedback, while irrigation shows stronger impacts during the day through latent heat flux feedback. Our comparison demonstrates the importance of irrigation in local and regional climate, highlighting the necessity of considering such land management practices in future assessments of regional climate change and climate mitigation.

Keywords: land use – land cover change, climate modeling, land-atmosphere interaction, irrigation, CESM2

INTRODUCTION

It is widely recognized that land use/land cover change (hereafter referred to simply as land use) affects the overlying atmosphere through land-atmosphere interactions, and thus modifies the local and broader-scale climate. The importance of land use in the climate system promoted the Coupled Model Intercomparison Project Phase 5 (CMIP5) to include land use forcing in its climate projections (Hurtt et al., 2011). Based on the CMIP5 simulations, many studies have been carried out to investigate the impacts of land use on climate (Brovkin et al., 2013; Kumar et al., 2013; Di Vittorio et al., 2014) and extreme events (Lejeune et al., 2017, 2018; Chen and Dirmeyer, 2018; Li et al., 2018). It is found that land use can have impacts comparable to increased greenhouse gasses or sea surface temperature variations for many climate variables (Avila et al., 2012; de Noblet-Ducoudré et al., 2012), and land-use forcing can be as important as other anthropogenic forcings

in explaining the historical changes in temperature extremes over the regions with extensive land use (Chen and Dirmeyer, 2018).

Besides land use, which usually refers to conversions from one land cover to another due to human activities, land management practices and their climatic impacts have drawn increasing attention recently (Luyssaert et al., 2014; Mahmood et al., 2014). As an important agricultural practice to maintain adequate soil moisture for stable crop production, irrigation not only modifies the surface water budget, but also affects the energy balance of the land surface, thereby altering the climate (Kueppers et al., 2007). For instance, irrigation can change surface partitioning of available energy between sensible and latent heat fluxes by allowing more evapotranspiration through increased soil moisture and larger vegetation coverage, potentially lowering near-surface temperatures over the irrigated areas.

Recent modeling studies have demonstrated the significant impacts of irrigation on near-surface climate and atmospheric circulation (e.g., Boucher et al., 2004; Kueppers et al., 2007; Lobell et al., 2009; Sacks et al., 2009; Lo and Famiglietti, 2013; Wei et al., 2013; Lu and Kueppers, 2015; de Vrese et al., 2016; Huang and Ullrich, 2016; Krakauer et al., 2016), especially the strong cooling effects on daytime temperatures or hot extremes. It is proposed that irrigation can be an effective way to mitigate the regional warming of hot extremes (Hirsch et al., 2017; Thiery et al., 2017). Studies based on satellite observations also indicate the substantial local cooling of irrigation (Ambika and Mishra, 2019; Chen and Dirmeyer, 2019b), and imply that the cooling effects may be underestimated by global climate models due to their coarse spatial resolutions (Sorooshian et al., 2011; Chen and Dirmeyer, 2019b).

Despite its fundamental importance in altering the regional climate, the full scope of land management has rarely been considered in recent climate assessment projects. For instance, CMIP5 did not include irrigation as a historical forcing (Kumar et al., 2013), and many of the participating Earth system models did not implement irrigation schemes in their land surface models (Singh et al., 2018). The project Land-Use and Climate, Identification of Robust Impacts (LUCID), for example, is mainly focused on the biogeophysical impacts of historical land use (de Noblet-Ducoudré et al., 2012). There are a few studies demonstrating the siginifance of irrigation compared to other land surface changes. For instance, the effects of irrigation on water vapor flows are equally as important as deforestation (Gordon et al., 2005); the cooling of irrigation is most pronounced compared to increased leaf area index and reduced tillage (Lobell et al., 2006). However, few studies have investigated the impacts of irrigation and its relative importance compared to historical land use in modifying local and regional temperatures.

With the goal of comparing these two types of land management, this study uses a state-of-the-art Earth system model, Community Earth System Model version 2 (CESM2), to investigate the separate impacts of land use and irrigation on summer temperatures and extreme heat events. We focus on boreal summer temperature because of the strong land-atmosphere interactions and high irrigation demands during the warm season, when these two land surface forcings should have the most profound climatic impacts and the greatest social implications.

METHODOLOGY

Land-Use Experiments in CESM2

The land-use experiments are conducted with CESM2, which is a coupled Earth System model composed of separate climate system components for atmosphere, ocean, land, sea ice and land ice. The major focus of this study is on the interactions between the land surface and atmosphere, so only the Community Atmosphere Model (CAM6) and Community Land Model (CLM5) components are used in our simulations (no interactive ocean or sea ice), with the component set F2000climo at a spatial resolution of $0.9° \times 1.25°$. The F2000climo component set allows climatology simulations with cyclic circa-year-2000 forcing, in which there are prescribed sea surface temperature (SST) and sea ice cover with a fixed CO_2 concentration of 367.0 ppm. Monthly mean climatology of SST and sea ice cover are derived from a merged product based on the monthly mean Hadley Center Sea Ice and SST dataset, version 1 (HadISST1), and version 2 of the NOAA weekly Optimum Interpolation SST (OISST2) analysis during the period 1995–2005 (Hurrell et al., 2008). Compared with the previous version of CLM, improvements are made in CLM5 to better represent soil and plant hydrology, snow density, carbon and nitrogen cycling and coupling, the representation of crops and human land management (Lawrence et al., 2019).

In CLM5, land surface heterogeneity is represented as a nested subgrid hierarchy, in which grid cells are composed of multiple land units (such as the vegetated unit and crop unit). The vegetated unit can be composed of different plant functional types (PFTs), and the crop unit can be composed of different crop functional types (CFTs). Land use is represented as the changes in percent PFTs and CFTs within a grid cell. In this study, two land-use experiments (*pre-industrial* and *present*) are carried out with prescribed pre-industrial and present land cover conditions (**Table 1**). The difference between *present* and *pre-industrial* can be considered as the impacts of historical land use. A two-tailed Student's t-test is conducted to assess the significance of the land-use induced difference. Details of the pre-industrial land cover can be found in Hurtt et al. (2006) and Lawrence et al. (2012), while the present land cover is derived from MODIS satellite data as described in Lawrence and Chase (2007).

Irrigation in CLM5

In the CLM5, there are a total of 31 managed crop types (Lawrence et al., 2018). Each crop type has rainfed and irrigated

TABLE 1 | Experimental design in CESM2.

Name	Land cover	Irrigation scheme
pre-industrial	pre-industrial (1850)	off
present	present (2015)	off
irrig	present (2015)	on

CFTs, which are placed on separate soil columns. The proportion of irrigated CFTs is based on a dataset of areas equipped for irrigation (Portmann et al., 2010), which is shown in **Figure 1D**. When irrigation is enabled, the model checks if the crops need irrigation in the first time step after 6 AM local time every day. If the crop leaf area is greater than zero and the available soil water is below a specified threshold, irrigation will be triggered. Irrigated water is removed from river water storage and applied directly to the ground surface. Details of the irrigation scheme in CLM5 can be found in Lawrence et al. (2018). To separate the impacts of land use and land management, an irrigation experiment, *irrig*, is carried out with the present land cover conditions (**Table 1**). Irrigation is not automatically activated in the *pre-industrial* and *present* experiments, so the difference between *irrig* and *present* can be considered as the effects of irrigation. A two-tailed Student's *t*-test is used to assess the significance of the irrigation induced difference.

Because the prognostic biogeochemical model is activated to estimate the vegetation phenology, land initial conditions for each experiment are obtained from a separate 700−year offline spin−up run, then each experiment is conducted for 60 years with output saved at three-hourly intervals.

Indices of Hot Extremes

Previous studies suggest that land use and irrigation have significant impacts on hot extremes (Avila et al., 2012; Pitman et al., 2012; Christidis et al., 2013; Hirsch et al., 2017; Thiery et al., 2017). Therefore, we assess the changes in four warm extreme temperature indices, listed and defined in **Table 2**, as recommended by the CCl/CLIVAR/JCOMM Expert Team on Climate Change Detection and Indices (ETCCDI; Alexander et al., 2006). These indices are based on daily maximum and minimum temperature and are developed to assess the intensity and frequency of extreme temperature events.

Additionally, to understand the mechanism of temperature responses to changes in land use and land management, other land surface variables (such as surface fluxes and radiation) are also included in our analysis. With the focus on daily minimum and maximum temperature, we identify the timing of daily maximum (minimum) land surface temperatures (T_s) based on three-hourly model output, and extract the corresponding surface fluxes and radiation when T_s reaches the daily maximum (minimum).

RESULTS

Historical Land Use and Irrigation Activities

Figures 1A–C shows the historical land cover change from pre-industrial to present day over the Northern Hemisphere. Deforestation has mainly occurred in the Midwest of the US, eastern Europe, India, eastern China, and in tropical areas such as Central America, Africa, and southeastern Asia. Most of the deforestation is driven by agricultural demand through cropland expansion in the middle latitudes, which has also led to grassland loss in such regions as the Great Plains, Eastern Europe,

TABLE 2 | Temperature indices used in this study.

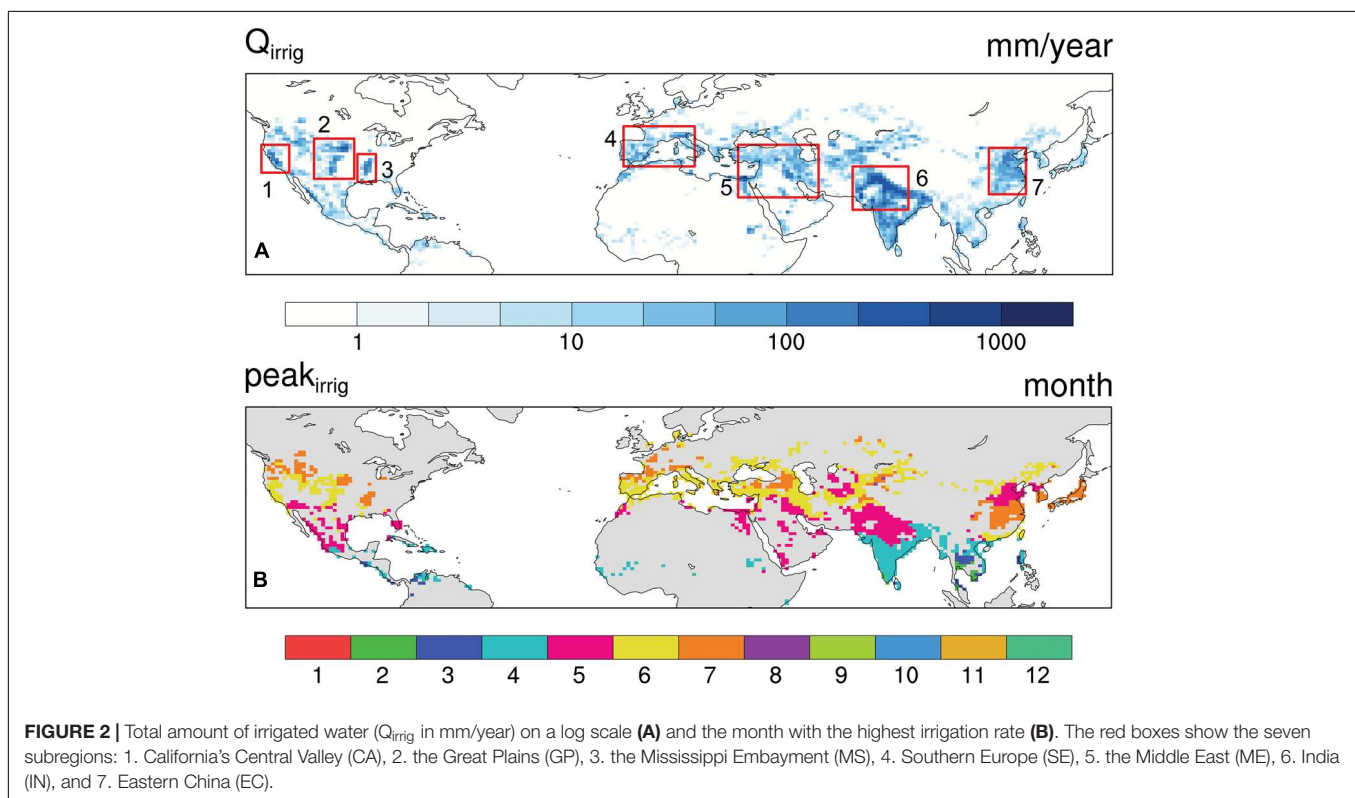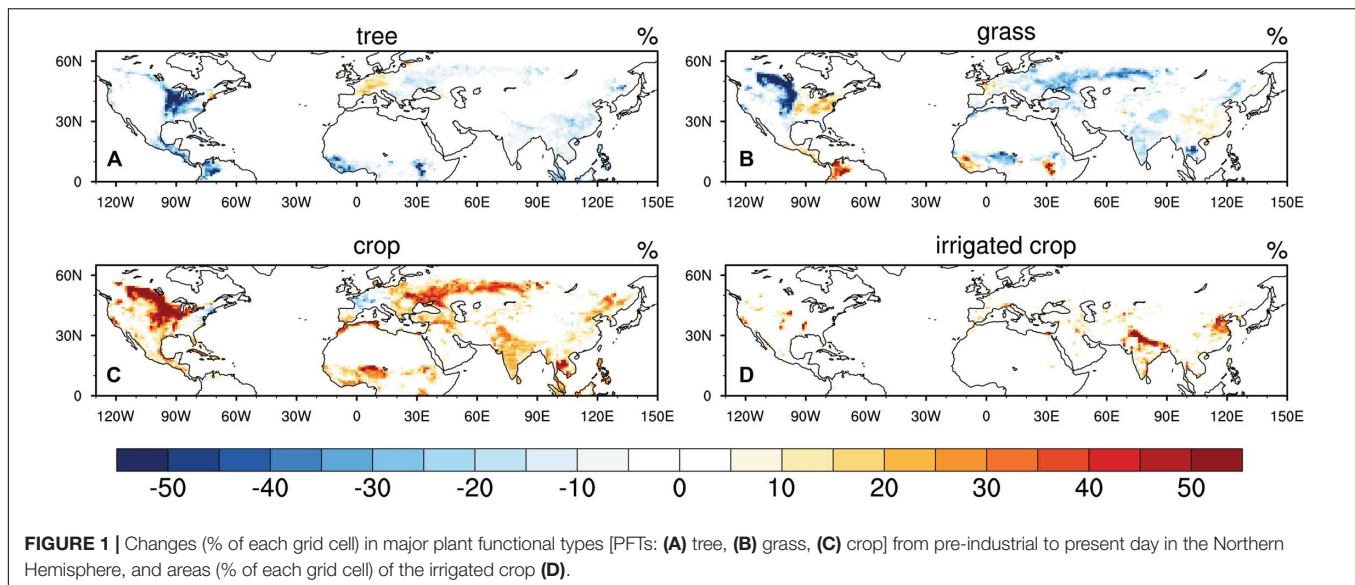| Index	definition	Unit
TXx	The warmest day of the year	K
TNx	The warmest night of the year	K
TX90p	Number of days when TX > 90th percentile	days
TN90p	Number of days when TN > 90th percentile	days

TX is daily maximum temperature, and TN is daily minimum temperature. Definitions of these indices can be found at http://etccdi.pacificclimate.org/list_27_indices.shtml (Karl et al., 1999; Peterson et al., 2001).

and India. Meanwhile, the conversion of cropland back into forest or grassland occurs in some regions of the northeastern US and western Europe. Grassland degradation (conversion of grassland into bare ground) is found in some regions of the Tibetan Plateau, which might be associated with over-stocking (Li et al., 2013).

Areas of the irrigated cropland are shown in **Figure 1D**. The irrigation systems are mainly distributed in northern India, eastern China, the Middle East, Southern Europe, the Central Valley in California, the North American Great Plains, and the Mississippi Embayment, according to Portmann et al. (2010). Based on the irrigation experiment, the total amount of irrigated water can be estimated in CLM5 (**Figure 2A**), which shows good agreement with observationally based estimates (Thiery et al., 2017), indicating that CESM2 is an appropriate tool to investigate the impact of irrigation (Huang and Ullrich, 2016; Thiery et al., 2017). Seven subregions with high irrigation rates are selected for regional analysis. We also identified the month with the highest irrigation rate (**Figure 2B**). Summertime peak irrigation occurs mostly in the middle latitudes, such as North America, the Mediterranean, and western/eastern Asia. In the tropics and regions that are influenced by monsoons (such as the East Asian Monsoon and North American Monsoon), the highest irrigation rate is mainly found in spring, which is the dry season prior to the onset monsoon rains. However, there is still a large amount of irrigated water applied during the summer in those regions, according to the irrigation algorithm in CLM5 (**Supplementary Figure S1**), exerting impacts on the surface climate then as well.

Changes in Temperature

Due to possible different responses of daytime temperature to deforestation at the land surface (T_s) and 2-m air (T_{2m}) reported in our previous work (Chen and Dirmeyer, 2019a), we present the results of T_s and T_{2m} separately (**Figure 3**). Historical deforestation leads to a significant daytime warming at the land surface (T_s) in the tropics, India, and the central US (**Figure 3A**). However, the change in daily maximum T_{2m} largely depends on the type of land use. Cooling effects on T_{2m} are found in parts of the central US, Central America and Columbia, where the major land use is the conversion of forest into cropland and grassland. For regions like India and Southeast Asia where forest and grassland are converted into cropland, there is increased daily maximum T_{2m}. In eastern Europe, the combined effects of deforestation and grassland conversion do

FIGURE 1 | Changes (% of each grid cell) in major plant functional types [PFTs: **(A)** tree, **(B)** grass, **(C)** crop] from pre-industrial to present day in the Northern Hemisphere, and areas (% of each grid cell) of the irrigated crop **(D)**.

FIGURE 2 | Total amount of irrigated water (Q_{irrig} in mm/year) on a log scale **(A)** and the month with the highest irrigation rate **(B)**. The red boxes show the seven subregions: 1. California's Central Valley (CA), 2. the Great Plains (GP), 3. the Mississippi Embayment (MS), 4. Southern Europe (SE), 5. the Middle East (ME), 6. India (IN), and 7. Eastern China (EC).

not result in significant changes to either T_s or T_{2m}. In eastern China, although there is no significant change in daily maximum T_s, land use can significantly decrease daily maximum T_{2m}. Conversion of grassland into cropland over the Great Plains tends to substantially decrease both daily maximum T_s and T_{2m}. Additionally, grassland degradation in the Tibetan Plateau leads to significant warming.

During the night, there are consistent changes in T_s and T_{2m} (**Figures 3E,G**), which show a similar pattern to the changes in

daily maximum T_s (**Figure 3A**). Significant cooling is found in the Great Plains and eastern Europe, while warming land surface and 2-m air are found in a majority of the deforested areas.

Irrigation activities can lead to a significant cooling at both the land surface and the 2-m air throughout the day, with greater changes in daytime temperatures. The cooling effects are more local, but comparable to (and even stronger than) the impacts of the historical land use. **Table 3** shows the regional changes in daily maximum and monthly mean T_{2m} and T_s due to historical

FIGURE 3 | Changes in summer daily maximum **(A–D)** and minimum **(E–H)** land surface temperature (T_s in K) and 2-m air temperature (T_{2m} in K) due to historical land use (left) and irrigation (right). Stippling indicates significance at the 95% confidence level.
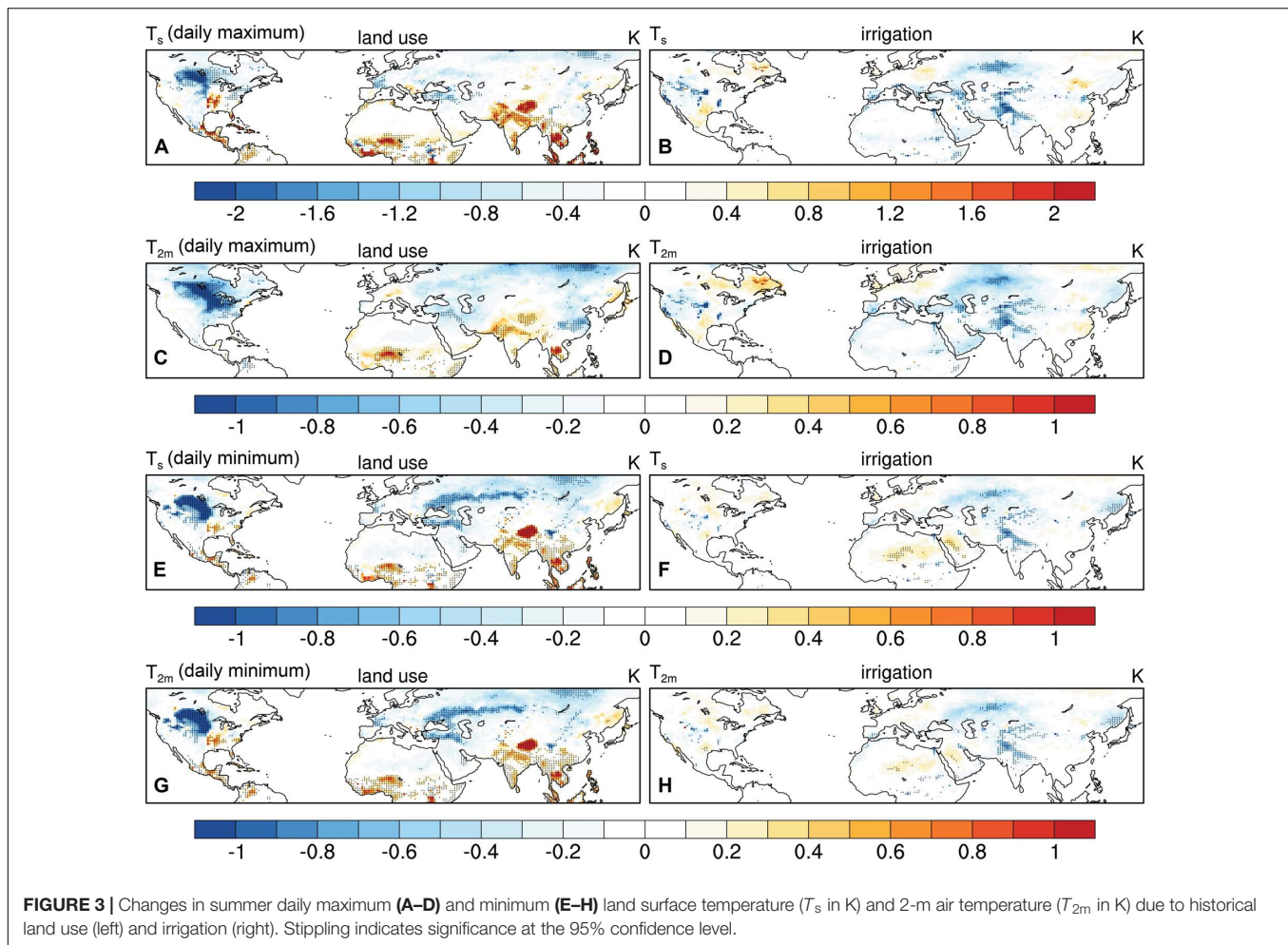
TABLE 3 | Regional average temperature changes due to land use and irrigation in the irrigated grid cells (with total summertime irrigation greater than 30 mm) in seven sub-regions. Bold numbers indicate over half of the grid cells have statistically significant temperature changes at the 95% confidence level.

Sub-regions		CA	GP	MS	SE	ME	IN	EC
No. of grid cells		11	25	11	20	37	33	43
Q_{irrg} (mm)	irrigation	77.23	73.88	86.14	50.17	47.17	42.27	46.96
T_{2m} daytime(K)	land use	**−0.24**	**−0.73**	**−0.76**	−0.12	**−0.42**	**0.48**	−0.19
	irrigation	**−1**	**−0.81**	**−0.38**	−0.36	**−0.65**	**−0.51**	**−0.58**
T_s daytime (K)	land use	0.03	**−1.66**	**0.79**	−0.4	**−0.5**	**1.26**	0.27
	irrigation	**−2.12**	**−1.46**	**−0.88**	**−0.87**	**−1.29**	**−1.41**	**−0.95**
T_{2m} monthly (K)	land use	**−0.31**	**−0.8**	0.1	−0.14	**−0.46**	**0.48**	−0.01
	irrigation	**−0.8**	**−0.52**	−0.16	−0.23	**−0.48**	**−0.51**	**−0.49**
T_s monthly (K)	land use	−0.24	**−1.1**	**0.55**	−0.22	**−0.52**	**0.68**	0.13
	irrigation	**−1.19**	**−0.71**	−0.31	−0.4	**−0.7**	**−0.88**	**−0.61**

land use and irrigation in the irrigated regions, where land use usually also occurs during the historical period. For instance, the local cooling by irrigation can be up to 2.1 K on daily maximum T_s and 1.0 K on T_{2m} in California. In India, land use leads to significant land surface warming (about 1.3 K), while irrigation cools local temperature by 1.4 K. Only in the Mississippi Embayment and Great Plains does land use show greater impacts on daily maximum or monthly mean 2-m air

than irrigation. In southern Europe, because of the mixed land use (both increased and decreased cropland) and relatively fewer areas with irrigation (**Figures 1C,D**), significant change is only manifested in the irrigation impacts on daily maximum T_s. There are also areas of warming away from the irrigated regions, which result from shifts in the general circulation driven by irrigation. Broader atmospheric effects are discussed further in section "Changes above the surface."

Changes in Surface Fluxes

To understand the mechanism of the temperature responses, we investigate the changes in the diurnal cycle of surface fluxes (**Figure 4** for daytime and **Figure 5** for nighttime). During the daytime, there is increased latent heat flux (LE) and decreased sensible heat flux (H) in the regions with the conversion of grassland to cropland (**Figure 4A**), such as the northern Great Plains, Eastern Europe, and northeastern China, where there is decreased T_s (**Figure 3A**). Increased LE is also found in the afforested regions, such as the northeastern US and western Europe, where there is a slight cooling at the land surface. In most areas of the tropics, deforestation leads to significantly decreased LE, suggesting the less evapotranspiration and consequently more H (**Figure 4C**) over the open land than the forest, resulting in a warming effect at the land surface (**Figure 3A**). However, in the United States Midwest, there is an evident decrease in H mainly due to decreased surface roughness after deforestation, which can explain the warming land surface but cooling of the air (**Figures 3A,C**).
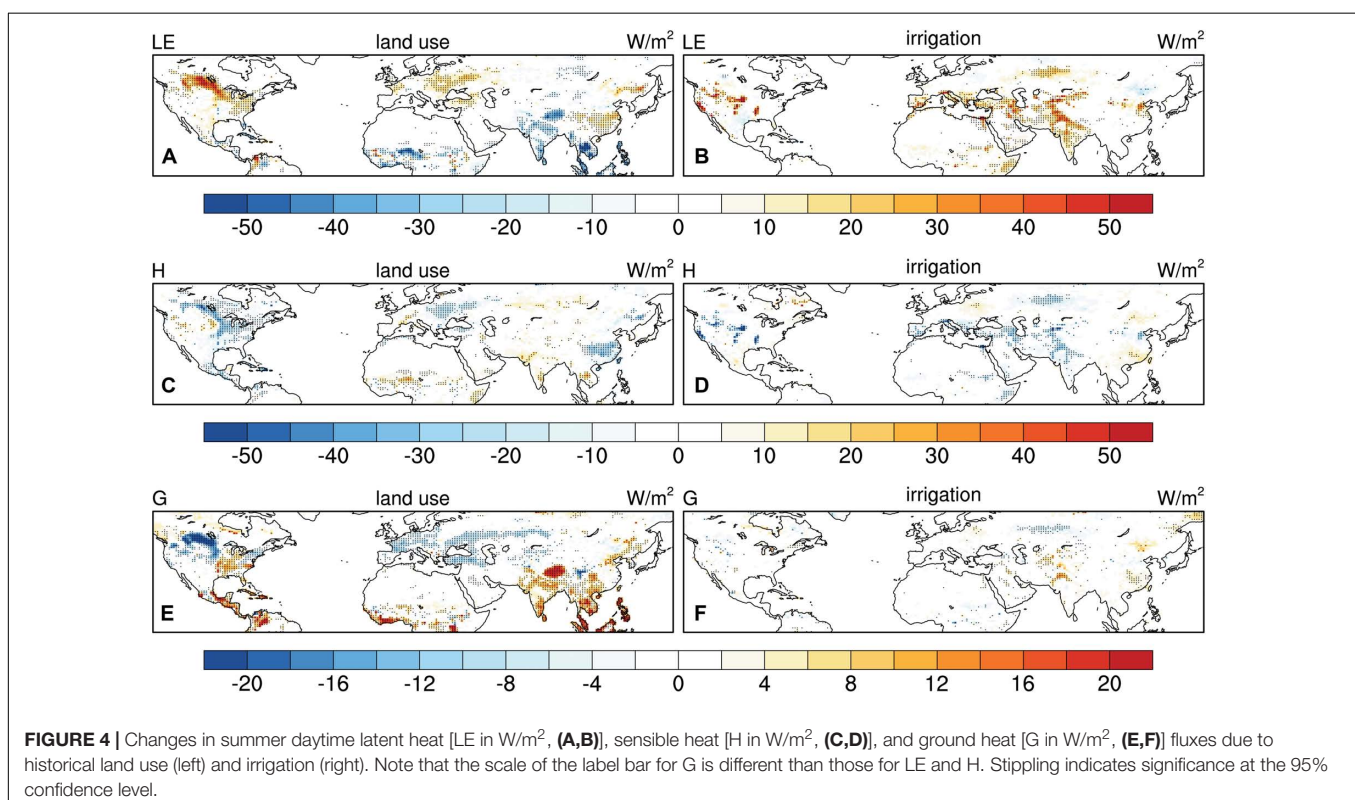
Compared to LE and H, ground heat flux (G) responds to land use with relatively small magnitudes during the daytime. Therefore, its change is not a major factor influencing the daytime temperature change. Generally, deforestation leads to more heat flux stored in the ground, while afforestation or grassland conversion results in a reduction of heat entering the ground because of more surface available energy being used as latent heat flux. During nighttime, there is an upward ground heat flux. In other words, the heat stored in the soil layers during the daytime can feed back to the land surface and enter the
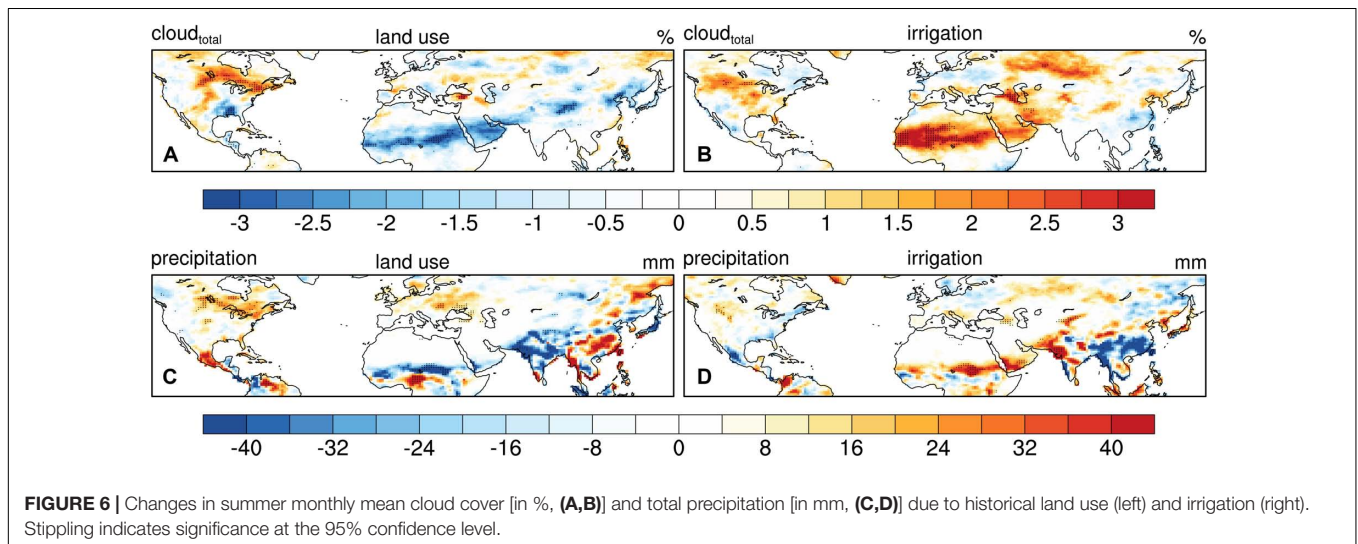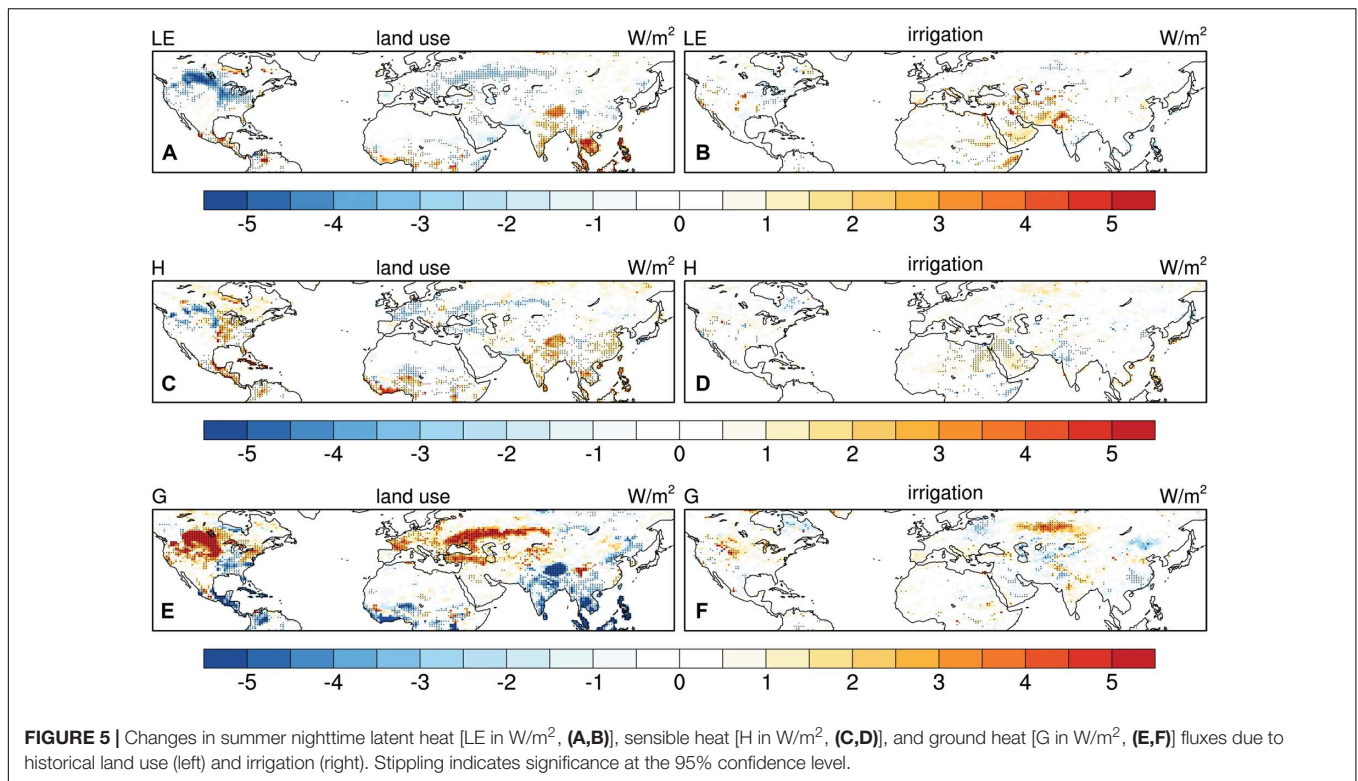
lower atmosphere. Therefore, changes in G show opposite signs during the daytime and nighttime (**Figures 4E, 5E**), and the nighttime T_s and T_{2m} (**Figures 3E,G**) are mainly determined by the changes in G.

Compared with land use, irrigation leads to consistently increased latent heat flux and decreased sensible heat flux throughout the day in the irrigated areas, especially in the Great Plains, California, and northwestern India (**Figures 5B,D, 6B,D**). Reduced T_s and T_{2m} are mainly associated with the evaporative cooling of irrigation.

Changes Above the Surface

Land use and land management do not only modify the local land surface features; they are also able to influence the atmosphere and large-scale circulation. Therefore, the temperature changes (especially for T_{2m}) can also be associated with the atmospheric feedback to land use or land management. **Figure 6** shows the changes in summer total cloud cover and precipitation due to land use and irrigation. Land use leads to a significant increase in cloud cover and precipitation over the northern plains of North America and parts of eastern Europe, which corresponds to the cooling effects in those regions. A significant decrease in cloud cover and precipitation is found in northern India and tropical Africa, which corresponds to the land use-induced warming effects in those regions. Irrigation generally increases cloud cover in many regions, possibly due to enhanced local convective processes, but the significant increase in precipitation is only found in northwestern India and limited regions of the Great
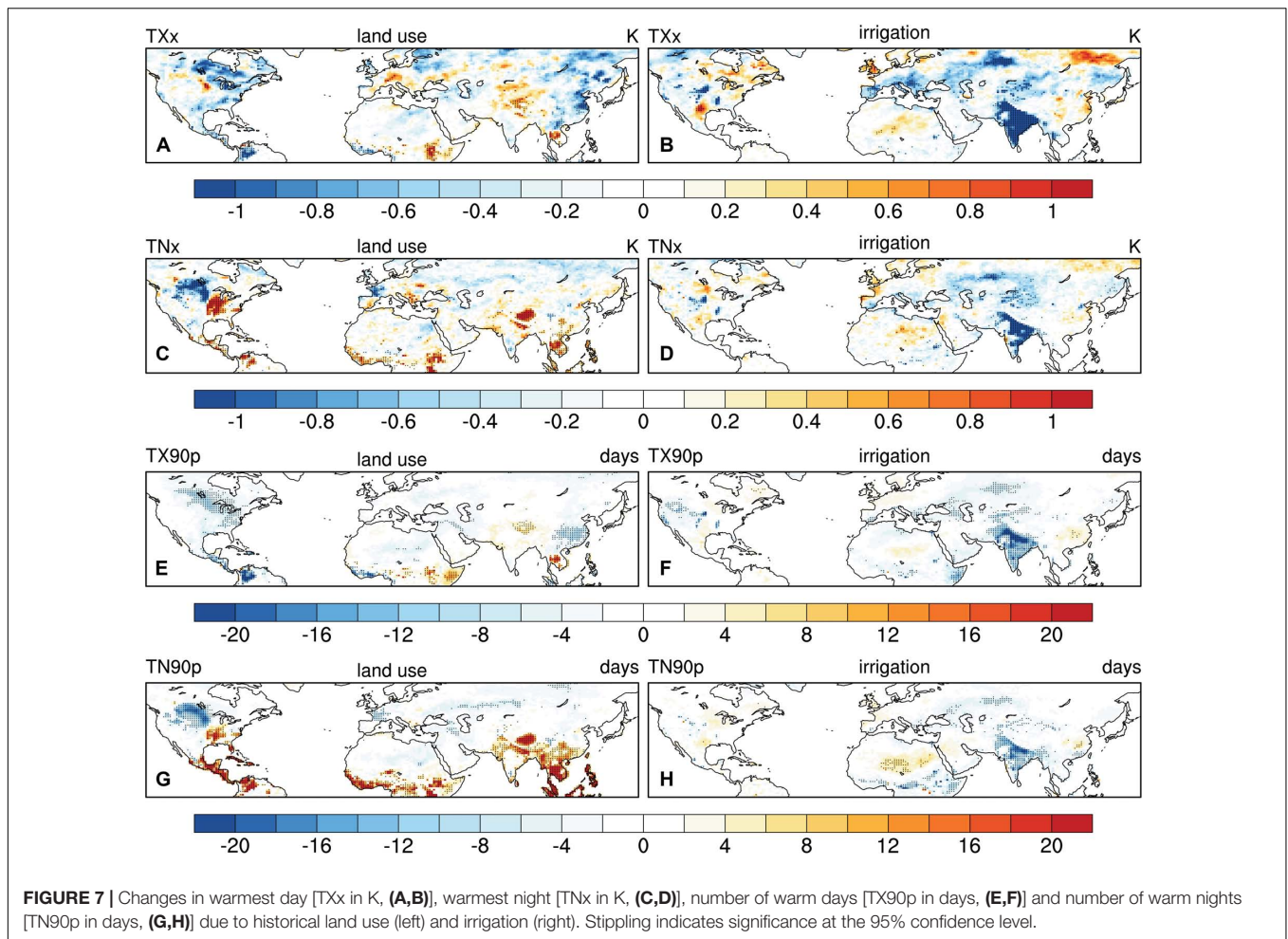

FIGURE 4 | Changes in summer daytime latent heat [LE in W/m², **(A,B)**], sensible heat [H in W/m², **(C,D)**], and ground heat [G in W/m², **(E,F)**] fluxes due to historical land use (left) and irrigation (right). Note that the scale of the label bar for G is different than those for LE and H. Stippling indicates significance at the 95% confidence level.

FIGURE 5 | Changes in summer nighttime latent heat [LE in W/m^2, **(A,B)**], sensible heat [H in W/m^2, **(C,D)**], and ground heat [G in W/m^2, **(E,F)**] fluxes due to historical land use (left) and irrigation (right). Stippling indicates significance at the 95% confidence level.

FIGURE 6 | Changes in summer monthly mean cloud cover [in %, **(A,B)**] and total precipitation [in mm, **(C,D)**] due to historical land use (left) and irrigation (right). Stippling indicates significance at the 95% confidence level.

Plains in the United States, which exhibit significant cooling effects of irrigation.

Although the changes in large-scale circulation and remote effects of land use/land management are not the scope of this study, the evident atmospheric feedback certainly demonstrates the impacts of land surface change on temperature through land-atmosphere interactions. For instance, the conversion of grassland into cropland in the northern plains of North America enhances evapotranspiration at the land surface, which exerts cooling effects based on the surface energy budget. On the other hand, higher evapotranspiration may lead to more cloud cover, which in turn decreases surface and near-surface temperature, and also potentially enhances precipitation, which further increases soil moisture and surface evapotranspiration.

Changes in Hot Extremes

We also examine the changes in hot extremes due to land use and land management (**Figure 7**). Generally, deforestation slightly reduces the intensity and frequency of hot events in middle latitudes during daytime, but leads to evidently more intense and frequent hot events during nighttime. The conversion of grassland into cropland, especially in the northern plains, shows

FIGURE 7 | Changes in warmest day [TXx in K, **(A,B)**], warmest night [TNx in K, **(C,D)**], number of warm days [TX90p in days, **(E,F)**] and number of warm nights [TN90p in days, **(G,H)**] due to historical land use (left) and irrigation (right). Stippling indicates significance at the 95% confidence level.

significantly reduced hot extremes. On the contrary, the impacts of irrigation on hot extremes are more evident during daytime. Significantly reduced hot extremes are found in the irrigated regions (except eastern China), where the irrigation-induced cooling can be stronger than the land-use impacts. It should be noted that maximum temperature in India occurs in late spring before the monsoon when there is a high irrigation demand. Therefore, strong cooling effects are found in this region, but are not manifested in the summertime temperature responses discussed in previous sections.

DISCUSSION AND CONCLUSION

This study presents a comparison between land use and irrigation with respect to their impacts on summer temperatures. Tropical deforestation shows an evident warming effect, especially at the land surface and during the nighttime. However, land-use impacts in the middle latitudes are dominated by the cooling effect of grassland conversion, while the extensive deforestation in the United States Midwest does not show strong impacts on local or regional temperature. A few caveats should be noted regarding the deforestation-temperature relationship.

First, uncertainties still remain in current land surface models in representing the energy partitioning between latent and sensible heat flux (Chen et al., 2018; Cai et al., 2019). Unlike the observed decrease in ET after deforestation (Meier et al., 2018), the models suggest a slight increase in latent heat flux (**Figure 4A**), consequently exerting a cooling effect. Second, the model suggests a warmer land surface but cooler air mainly due to the decreased sensible heat flux after deforestation. The conversion of forest lands to agriculture reduces surface roughness and increases aerodynamic resistance, so the heat transfer becomes less efficient over the open land (Chen and Dirmeyer, 2019a). Consequently, less efficient turbulent heat exchange with the atmosphere leads to land surface warming (**Figure 3A**) but cooling of the lower-atmosphere (**Figure 3C**). The dominance of surface roughness (or aerodynamic resistance) in deforestation-induced biophysical effects has been documented in previous studies (Liao et al., 2018; Winckler et al., 2019a). The different responses in T_s and T_{2m} to deforestation are also found in another climate model (Winckler et al., 2019a). However, further assessments of land-use impacts on temperature are necessarily taken using multi-model experiments, such as The Land Use Model Intercomparison Project [LUMIP, (Lawrence et al., 2016)]. Furthermore, observation-based studies suggest

nighttime cooling (Schultz et al., 2017; Liao et al., 2018), which can be attributed to the decreased turbulence after deforestation and less heat aloft being brought to the surface (Lee et al., 2011). However, our results suggest nighttime warming of deforestation, which is mainly driven by the heat storage in the ground. Similar nighttime warming is also shown in other climate models (Vanden Broucke et al., 2015; Winckler et al., 2019b), suggesting ground heat flux and the nocturnal boundary layer need further attention in future model evaluation and development.

Meanwhile, a strong cooling effect is found in the irrigated areas, especially during the daytime and at the land surface. For instance, irrigation in California reduces daytime T_s by over 2 K. Such a cooling effect of irrigation is even greater than the land-use impacts in many regions (**Table 2**). Even though the irrigation-induced cooling is also confirmed through ground-based and satellite observations (Bonfils and Lobell, 2007; Lobell et al., 2008; Chen and Dirmeyer, 2019b), caution should be taken to interpret the simulated irrigation effects. The local cooling of irrigation can be even stronger if the model is run at a higher spatial resolution (Kueppers et al., 2007; Lobell et al., 2009; Sacks et al., 2009; Lo and Famiglietti, 2013; Lu and Kueppers, 2015; Huang and Ullrich, 2016; Chen and Dirmeyer, 2019b). For instance, there is up to 7 K of cooling due to irrigation over California based on a regional climate model (e.g., Kueppers et al., 2007), which highlights the impacts of irrigation at local or regional scales.

It also should be noted that uncertainties exist in current irrigation simulations. Observation-based studies suggest a nighttime warming in irrigated areas (Kanamaru and Kanamitsu, 2008; Chen and Jeong, 2018) because irrigation increases soil heat capacity (Kalnay and Cai, 2003) and thermal conductivity (Kanamaru and Kanamitsu, 2008), which allows more heat to be stored during daytime and released from the ground to the air during nighttime. Meanwhile, elevated moisture of the air would enhance downward longwave radiation, which would have a warming effect especially during night (Souri et al., 2020). In our results, although increased ground heat flux (implying more heat entered into the soil) is evident in the irrigated areas during daytime (**Figure 4F**), decreased ground heat flux (implying more heat released from the ground) is not found during nighttime (**Figure 5F**), and irrigation leads to a slight cooling in daily minimum temperature (**Figures 3F,H**). The issue with the simulated response of minimum temperature to irrigation has also been documented in other model-based studies (Kueppers et al., 2008; Huang and Ullrich, 2016). As ground heat flux is calculated from the residual of the surface energy balance in order to precisely conserve energy (Lawrence et al., 2018), the model bias may be associated with the uncertainties in surface flux parameterization in land surface models. The uncertainties in the representation of irrigation characteristics are also documented in other climate models, such as the Max Planck Institute for Meteorology's Earth System model (MPI-ESM), and regional climate models. The irrigation-induced temperature change can be highly related to the land-atmosphere coupling scheme used in the model, irrigation effectiveness, timing of irrigation (de Vrese and Hagemann, 2017). Kueppers et al. (2008) also found that the simulated effects of irrigation vary

among different regional climate models due to different model physics and irrigation parameterizations. These factors should to considered in future assessments of irrigation impacts, and multiple-model approaches are necessary to further evaluate the uncertainties in the representation of irrigation in different Earth system models.

Additionally, there are possibly remote impacts of land use or irrigation on climate beyond the regions where the land use and land management occur. For instance, there are evident changes in temperature (**Figure 3**), evapotranspiration (**Figure 4**), cloud cover (**Figure 6**) in the northeast of Caspian Sea, although irrigation is only applied in the south of this region. Such a non-local effect of irrigation is also shown in previous studies using different climate models (e.g., Puma and Cook, 2010). Although many studies have discussed the remote effects of land use and land management (e.g., Wei et al., 2013; Badger and Dirmeyer, 2016; de Vrese et al., 2016; Swann et al., 2018), the detected remote effects can be influenced by many factors, such as the length of simulations (Swann et al., 2018), representation of ocean circulation (Badger and Dirmeyer, 2016; Krakauer et al., 2016), and model physics (de Vrese et al., 2016), which need further investigation in future studies.

Our results mainly present the climatic impacts of land use and land management during summer because of the strong land-atmosphere interactions and intensive agricultural practices in the warm season. We acknowledge land cover change also has significant impacts on temperature during winter, especially for boreal deforestation, which exerts a cooling effect through snow-albedo effects (Davin and de Noblet-Ducoudré, 2010); irrigation also occurs in winter in some regions and has the potential to alter temperature then (Chen and Jeong, 2018). **Supplementary Figure S2** shows a significant cooling in the deforested areas in the United States Midwest and Northern Plains and a significant warming effect of tropical deforestation during the boreal winter. However, no evident change in surface temperature is found in the irrigation regions in this study.

As the goal of this paper is to emphasize the relative importance of land management in regional climate (Thiery et al., 2017) and the implications in hot extreme adaptation under the background of global climate change (Hirsch et al., 2017), our results suggest that the local cooling effects of irrigation can be as strong as the land-use impacts during the boreal summer. As the cropland area is projected to continue growing in all the shared socioeconomic pathways (SSPs) in CMIP6 and about a half of the SSP scenarios suggest an increase in irrigated cropland area in the future (Lawrence et al., 2016), the importance of land management in local and regional climate will be amplified by potentially intensified irrigation activities under a warming climate. Additionally, considering the enhanced ET due to irrigation (**Figure 4B**), which can potentially raise wet-bulb temperatures (Kang and Eltahir, 2018), humidity should also be considered in future assessments of irrigation impacts on heat waves and their social impacts.

In summary, this study highlights the importance of irrigation in local and regional climate based on the experiments using the most recent version of CESM. It should be noted that other land management practices, such no-till farming

(Davin et al., 2014) or cover crops (Lombardozzi et al., 2018), may also have certain climatic consequences from the biogeophysical perspective through radiative processes. Also, there are many approaches to irrigation (e.g., surface irrigation, sprinklers including center-pivot irrigation, drip irrigation) drawing from both surface water and groundwater. Current models do not represent this variety, yet each has different potential effects on soil moisture and surface fluxes including evaporative cooling. Therefore, toward a comprehensive understanding of the climatic impacts of land management, different agricultural practices should be considered and compared when assessing regional-scale climate adaptation and mitigation (Lobell et al., 2006; Seneviratne et al., 2018).

DATA AVAILABILITY STATEMENT

The datasets generated for this study are available on request to the corresponding author.

AUTHOR CONTRIBUTIONS

LC and PD designed the study. LC performed the model simulations and the data analysis. Both authors contributed to the writing of the manuscript.

SUPPLEMENTARY MATERIAL

The Supplementary Material for this article can be found online at: https://www.frontiersin.org/articles/10.3389/feart.2020.00245/full#supplementary-material

REFERENCES

Alexander, L. V., Zhang, X., Peterson, T. C., Caesar, J., Gleason, B., Klein Tank, A. M. G., et al. (2006). Global observed changes in daily climate extremes of temperature and precipitation. *J. Geophys. Res.* 111, 1–22. doi: 10.1029/2005JD006290

Ambika, A. K., and Mishra, V. (2019). Observational evidence of irrigation influence on vegetation health and land surface temperature in India. *Geophys. Res. Lett.* 46, 13441–13451. doi: 10.1029/2019GL084367

Avila, F. B., Pitman, A. J., Donat, M. G., Alexander, L. V., and Abramowitz, G. (2012). Climate model simulated changes in temperature extremes due to land cover change. *J. Geophys. Res.* 117:D04108. doi: 10.1029/2011JD016382

Badger, A. M., and Dirmeyer, P. A. (2016). Diagnosing nonlinearities in the local and remote responses to partial Amazon deforestation. *J. Geophys. Res. Atmos.* 121, 9033–9047. doi: 10.1002/2015JD024013

Bonfils, C., and Lobell, D. (2007). Empirical evidence for a recent slowdown in irrigation-induced cooling. *Proc. Natl. Acad. Sci. U.S.A.* 104, 13582–13587. doi: 10.1073/pnas.0700144104

Boucher, O., Myhre, G., and Myhre, A. (2004). Direct human influence of irrigation on atmospheric water vapour and climate. *Clim. Dyn.* 22, 597–603. doi: 10.1007/s00382-004-0402-4

Brovkin, V., Boysen, L., Arora, V. K., Boisier, J. P., Cadule, P., Chini, L., et al. (2013). Effect of anthropogenic land-use and land-cover changes on climate and land carbon storage in CMIP5 projections for the twenty-first century. *J. Clim.* 26, 6859–6881. doi: 10.1175/JCLI-D-12-00623.1

Cai, X., Riley, W. J., Zhu, Q., Tang, J., Zeng, Z., Bisht, G., et al. (2019). Improving representation of deforestation effects on evapotranspiration in the E3SM land model. *J. Adv. Model. Earth Syst.* 11, 2412–2427. doi: 10.1029/2018MS001551

Chen, L., and Dirmeyer, P. A. (2018). The relative importance among anthropogenic forcings of land use/land cover change in affecting temperature extremes. *Clim. Dyn.* 52, 1–17. doi: 10.1007/s00382-018-4250-z

Chen, L., and Dirmeyer, P. A. (2019a). Differing responses of the diurnal cycle of land surface and air temperatures to deforestation. *J. Clim.* 32, 7067–7079. doi: 10.1175/JCLI-D-19-0002.1

Chen, L., and Dirmeyer, P. A. (2019b). Global observed and modelled impacts of irrigation on surface temperature. *Int. J. Climatol.* 39, 2587–2600. doi: 10.1002/joc.5973

Chen, L., Dirmeyer, P. A., Guo, Z., and Schultz, N. M. (2018). Pairing FLUXNET sites to validate model representations of land-use/land-cover change. *Hydrol. Earth Syst. Sci.* 22, 111–125. doi: 10.5194/hess-22-111-2018

Chen, X., and Jeong, S.-J. (2018). Irrigation enhances local warming with greater nocturnal warming effects than daytime cooling effects. *Environ. Res. Lett.* 13:024005. doi: 10.1088/1748-9326/aa9dea

Christidis, N., Stott, P. A., Hegerl, G. C., and Betts, R. A. (2013). The role of land use change in the recent warming of daily extreme temperatures. *Geophys. Res. Lett.* 40, 589–594. doi: 10.1002/grl.50159

Davin, E. L., and de Noblet-Ducoudré, N. (2010). Climatic impact of global-scale deforestation: radiative versus nonradiative processes. *J. Clim.* 23, 97–112. doi: 10.1175/2009JCLI3102.1

Davin, E. L., Seneviratne, S. I., Ciais, P., Olioso, A., and Wang, T. (2014). Preferential cooling of hot extremes from cropland albedo management. *Proc. Natl. Acad. Sci. U.S.A.* 111, 9757–9761. doi: 10.1073/pnas.1317323111

de Noblet-Ducoudré, N., Boisier, J.-P., Pitman, A., Bonan, G. B., Brovkin, V., Cruz, F., et al. (2012). Determining robust impacts of land-use-induced land cover changes on surface climate over North America and Eurasia: results from the First Set of LUCID experiments. *J. Clim.* 25, 3261–3281. doi: 10.1175/JCLI-D-11-00338.1

de Vrese, P., and Hagemann, S. (2017). Uncertainties in modelling the climate impact of irrigation. *Clim. Dyn.* 51, 1–16. doi: 10.1007/s00382-017-3996-z

de Vrese, P., Hagemann, S., and Claussen, M. (2016). Asian irrigation, African rain: remote impacts of irrigation. *Geophys. Res. Lett.* 43, 3737–3745. doi: 10.1002/2016GL068146

Di Vittorio, A. V., Chini, L. P., Bond-Lamberty, B., Mao, J., Shi, X., Truesdale, J., et al. (2014). From land use to land cover: restoring the afforestation signal in a coupled integrated assessment–earth system model and the implications for CMIP5 RCP simulations. *Biogeosciences* 11, 6435–6450. doi: 10.5194/bg-11-6435-2014

Gordon, L. J., Steffen, W., Jönsson, B. F., Folke, C., Falkenmark, M., and Johannessen, A. (2005). Human modification of global water vapor flows from the land surface. *Proc. Natl. Acad. Sci. U.S.A.* 102, 7612–7617. doi: 10.1073/pnas.0500208102

Hirsch, A. L., Wilhelm, M., Davin, E. L., Thiery, W., and Seneviratne, S. I. (2017). Can climate-effective land management reduce regional warming? *J. Geophys. Res. Atmos.* 122, 2269–2288. doi: 10.1002/2016JD026125

Huang, X., and Ullrich, P. A. (2016). Irrigation impacts on California's climate with the variable-resolution CESM. *J. Adv. Model. Earth Syst.* 8, 1151–1163. doi: 10.1002/2016MS000656

Hurrell, J. W., Hack, J. J., Shea, D., Caron, J. M., and Rosinski, J. (2008). A new sea surface temperature and sea ice boundary dataset for the community atmosphere model. *J. Clim.* 21, 5145–5153. doi: 10.1175/2008JCLI2292.1

Hurtt, G. C., Chini, L. P., Frolking, S., Betts, R. A., Feddema, J., Fischer, G., et al. (2011). Harmonization of land-use scenarios for the period 1500–2100: 600 years of global gridded annual land-use transitions, wood harvest, and resulting secondary lands. *Clim. Change* 109, 117–161. doi: 10.1007/s10584-011-0153-152

Hurtt, G. C., Frolking, S., Fearon, M. G., Moore, B., Shevliakova, E., Malyshev, S., et al. (2006). The underpinnings of land-use history: three centuries of global gridded land-use transitions, wood-harvest activity, and resulting secondary lands. *Glob. Change Biol.* 12, 1208–1229. doi: 10.1111/j.1365-2486.2006.01150.x

Kalnay, E., and Cai, M. (2003). Impact of urbanization and land-use change on climate. *Nature* 423, 528–531. doi: 10.1038/nature01675

Kanamaru, H., and Kanamitsu, M. (2008). Model Diagnosis of Nighttime Minimum Temperature Warming during Summer due to Irrigation in the California Central Valley. *J. Hydrometeor.* 9, 1061–1072. doi: 10.1175/2008JHM967.1

Kang, S., and Eltahir, E. A. B. (2018). North China Plain threatened by deadly heatwaves due to climate change and irrigation. *Nat. Commun.* 9:2894. doi: 10.1038/s41467-018-05252-y

Karl, T. R., Nicholls, N., and Ghazi, A. (1999). "CLIVAR/GCOS/WMO workshop on indices and indicators for climate extremes workshop summary," in *Weather and Climate Extremes*, eds T. R. Karl, N. Nicholls, and A. Ghazi (Dordrecht: Springer Netherlands), 3–7. doi: 10.1007/978-94-015-9265-9_2

Krakauer, N. Y., Puma, M. J., Cook, B. I., Gentine, P., and Nazarenko, L. (2016). Ocean–atmosphere interactions modulate irrigation's climate impacts. *Earth Syst. Dynam.* 7, 863–876. doi: 10.5194/esd-7-863-2016

Kueppers, L. M., Snyder, M. A., and Sloan, L. C. (2007). Irrigation cooling effect: regional climate forcing by land-use change. *Geophys. Res. Lett.* 34:L03703. doi: 10.1029/2006GL028679

Kueppers, L. M., Snyder, M. A., Sloan, L. C., Cayan, D., Jin, J., Kanamaru, H., et al. (2008). Seasonal temperature responses to land-use change in the western United States. *Glob. Planet. Change* 60, 250–264. doi: 10.1016/j.gloplacha.2007.03.005

Kumar, S., Dirmeyer, P. A., Merwade, V., DelSole, T., Adams, J. M., and Niyogi, D. (2013). Land use/cover change impacts in CMIP5 climate simulations: a new methodology and 21st century challenges. *J. Geophys. Res. Atmos.* 118, 6337–6353. doi: 10.1002/jgrd.50463

Lawrence, D., Fisher, R., Koven, C., Oleson, K., Swenson, S., and Vertenstein, M. (2018). *Technical Description of version 5.0 of the Community Land Model (CLM)*. Andhra Pradesh: National Center for Atmospheric Research.

Lawrence, D. M., Fisher, R. A., Koven, C. D., Oleson, K. W., Swenson, S. C., Bonan, G., et al. (2019). The Community Land Model version 5: description of new features, benchmarking, and impact of forcing uncertainty. *J. Adv. Model. Earth Syst.* 11, 4245–4287. doi: 10.1029/2018MS001583

Lawrence, D. M., Hurtt, G. C., Arneth, A., Brovkin, V., Calvin, K. V., Jones, A. D., et al. (2016). The Land Use Model Intercomparison Project (LUMIP) contribution to CMIP6: rationale and experimental design. *Geosci. Model Dev.* 9, 2973–2998. doi: 10.5194/gmd-9-2973-2016

Lawrence, P. J., and Chase, T. N. (2007). Representing a new MODIS consistent land surface in the Community Land Model (CLM 3.0). *J. Geophys. Res.* 112:G01023. doi: 10.1029/2006JG000168

Lawrence, P. J., Feddema, J. J., Bonan, G. B., Meehl, G. A., O'neill, B. C., Oleson, K. W., et al. (2012). Simulating the Biogeochemical and Biogeophysical Impacts of Transient Land Cover Change and Wood Harvest in the Community Climate System Model (CCSM4) from 1850 to 2100. *J. Clim.* 25, 3071–3095. doi: 10.1175/JCLI-D-11-00256.1

Lee, X., Goulden, M. L., Hollinger, D. Y., Barr, A., Black, T. A., Bohrer, G., et al. (2011). Observed increase in local cooling effect of deforestation at higher latitudes. *Nature* 479, 384–387. doi: 10.1038/nature10588

Lejeune, Q., Davin, E. L., Gudmundsson, L., Winckler, J., and Seneviratne, S. I. (2018). Historical deforestation locally increased the intensity of hot days in northern mid-latitudes. *Nat. Clim. Chang.* 8, 386–390. doi: 10.1038/s41558-018-0131-z

Lejeune, Q., Seneviratne, S. I., and Davin, E. L. (2017). Historical land-cover change impacts on climate: comparative assessment of LUCID and CMIP5 multimodel experiments. *J. Clim.* 30, 1439–1459. doi: 10.1175/JCLI-D-16-0213.1

Li, X., Chen, H., Wei, J., Hua, W., Sun, S., Ma, H., et al. (2018). Inconsistent responses of hot extremes to historical land use and cover change among the selected CMIP5 models. *J. Geophys. Res. Atmos.* 123, 3497–3512. doi: 10.1002/2017JD028161

Li, X. L., Gao, J., Brierley, G., Qiao, Y. M., Zhang, J., and Yang, Y. W. (2013). Rangeland degradation on the qinghai-tibet plateau: implications for rehabilitation. *Land Degrad. Dev.* 24, 72–80. doi: 10.1002/ldr.1108

Liao, W., Rigden, A. J., and Li, D. (2018). Attribution of local temperature response to deforestation. *J. Geophys. Res. Biogeosci.* 123, 1572–1587. doi: 10.1029/2018JG004401

Lo, M.-H., and Famiglietti, J. S. (2013). Irrigation in California's Central Valley strengthens the southwestern U.S. water cycle. *Geophys. Res. Lett.* 40, 301–306. doi: 10.1002/grl.50108

Lobell, D., Bala, G., Mirin, A., Phillips, T., Maxwell, R., and Rotman, D. (2009). Regional differences in the influence of irrigation on climate. *J. Clim.* 22, 2248–2255. doi: 10.1175/2008JCLI2703.1

Lobell, D. B., Bala, G., and Duffy, P. B. (2006). Biogeophysical impacts of cropland management changes on climate. *Geophys. Res. Lett.* 33: L06708. doi: 10.1029/2005GL025492

Lobell, D. B., Bonfils, C. J., Kueppers, L. M., and Snyder, M. A. (2008). Irrigation cooling effect on temperature and heat index extremes. *Geophys. Res. Lett.* 35:L09705. doi: 10.1029/2008GL034145

Lombardozzi, D. L., Bonan, G. B., Wieder, W., Grandy, A. S., Morris, C., and Lawrence, D. L. (2018). Cover crops may cause winter warming in snow-covered regions. *Geophys. Res. Lett.* 45:024005. doi: 10.1029/2018GL079000

Lu, Y., and Kueppers, L. (2015). Increased heat waves with loss of irrigation in the United States. *Environ. Res. Let.* 10:064010. doi: 10.1088/1748-9326/10/6/064010

Luyssaert, S., Jammet, M., Stoy, P., Estel, S., Pongratz, J., Ceschia, E., et al. (2014). Land management and land-cover change have impacts of similar magnitude on surface temperature. *Nat. Clim. Chang.* 4, 389–393. doi: 10.1038/nclimate2196

Mahmood, R., Pielke, R. A. Sr., Hubbard, K. G., Niyogi, D., Dirmeyer, P. A., et al. (2014). Land cover changes and their biogeophysical effects on climate. *Int. J. Climatol.* 34, 929–953. doi: 10.1002/joc.3736

Meier, R., Davin, E. L., Lejeune, Q., Hauser, M., Li, Y., Martens, B., et al. (2018). Evaluating and improving the Community Land Model's sensitivity to land cover. *Biogeosciences* 15, 4731–4757. doi: 10.5194/bg-15-4731-2018

Peterson, T. C., Folland, C., Gruza, G., Hogg, W., Mokssit, A., and Plummer, N. (2001). *Report on the Activities of the Working Group on Climate Change Detection and Related Rapporteurs 1998-2001*. Geneve: WMO.

Pitman, A. J., de Noblet-Ducoudré, N., Avila, F. B., Alexander, L. V., Boisier, J.-P., Brovkin, V., et al. (2012). Effects of land cover change on temperature and rainfall extremes in multi-model ensemble simulations. *Earth Syst. Dynam.* 3, 213–231. doi: 10.5194/esd-3-213-2012

Portmann, F. T., Siebert, S., and Döll, P. (2010). MIRCA2000-Global monthly irrigated and rainfed crop areas around the year 2000: a new high-resolution data set for agricultural and hydrological modeling. *Global Biogeochem. Cycles* 24:GB1011. doi: 10.1029/2008GB003435

Puma, M. J., and Cook, B. I. (2010). Effects of irrigation on global climate during the 20th century. *J. Geophys. Res.* 115:D16120. doi: 10.1029/2010JD014122

Sacks, W. J., Cook, B. I., Buenning, N., Levis, S., and Helkowski, J. H. (2009). Effects of global irrigation on the near-surface climate. *Clim. Dyn.* 33, 159–175. doi: 10.1007/s00382-008-0445-z

Schultz, N. M., Lawrence, P. J., and Lee, X. (2017). Global satellite data highlights the diurnal asymmetry of the surface temperature response to deforestation. *J. Geophys. Res. Biogeosci.* 122, 903–917. doi: 10.1002/2016JG003653

Seneviratne, S. I., Phipps, S. J., Pitman, A. J., Hirsch, A. L., Davin, E. L., Donat, M. G., et al. (2018). Land radiative management as contributor to regional-scale climate adaptation and mitigation. *Nat. Geosci.* 11, 88–96. doi: 10.1038/s41561-017-0057-5

Singh, D., McDermid, S. P., Cook, B. I., Puma, M. J., Nazarenko, L., and Kelley, M. (2018). Distinct influences of land cover and land management on seasonal climate. *J. Geophys. Res. Atmos.* 123, 12017–12039. doi: 10.1029/2018JD028874

Sorooshian, S., Li, J., Hsu, K., and Gao, X. (2011). How significant is the impact of irrigation on the local hydroclimate in California's Central Valley? Comparison of model results with ground and remote-sensing data. *J. Geophys. Res.* 116:D06107. doi: 10.1029/2010JD014775

Souri, A. H., Wang, H., González Abad, G., Liu, X., and Chance, K. (2020). Quantifying the impact of excess moisture from transpiration from crops on an extreme heat wave event in the midwestern U.S.: a top-down constraint from moderate resolution imaging spectroradiometer water vapor retrieval. *J. Geophys. Res. Atmos.* 125:e2019JD031941. doi: 10.1029/2019JD031941

Swann, A. L. S., Laguë, M. M., Garcia, E. S., Field, J. P., Breshears, D. D., Moore, D. J. P., et al. (2018). Continental-scale consequences of tree die-offs in North America: identifying where forest loss matters most. *Environ. Res. Lett.* 13:055014. doi: 10.1088/1748-9326/aaba0f

Thiery, W., Davin, E. L., Lawrence, D. M., Hirsch, A. L., Hauser, M., and Seneviratne, S. I. (2017). Present-day irrigation mitigates heat extremes. *J. Geophys. Res. Atmos.* 122, 1403–1422. doi: 10.1002/2016JD025740

Vanden Broucke, S., Luyssaert, S., Davin, E. L., Janssens, I., and Lipzig, N. (2015). New insights in the capability of climate models to simulate the impact of LUC

based on temperature decomposition of paired site observations. *J. Geophys. Res. Atmos.* 120, 5417–5436. doi: 10.1002/2015JD023095

Wei, J., Dirmeyer, P. A., Wisser, D., Bosilovich, M. G., and Mocko, D. M. (2013). Where does the irrigation water go? an estimate of the contribution of irrigation to precipitation using MERRA. *J. Hydrometeor* 14, 275–289. doi: 10.1175/JHM-D-12-079.1

Winckler, J., Reick, C. H., Bright, R. M., and Pongratz, J. (2019a). Importance of surface roughness for the local biogeophysical effects of deforestation. *J. Geophys. Res. Atmos.* 124, 8605–8618. doi: 10.1029/2018JD030127

Winckler, J., Reick, C. H., Luyssaert, S., Cescatti, A., Stoy, P. C., Lejeune, Q., et al. (2019b). Different response of surface temperature and air temperature to deforestation in climate models. *Earth Syst. Dynam.* 10, 473–484. doi: 10.5194/esd-10-473-2019